IEEE Access
Multidisciplinary | Rapid Review | Open Access Journal

Received December 16, 2019, accepted December 29, 2019, date of publication January 9, 2020, date of current version January 16, 2020.

Digital Object Identifier 10.1109/ACCESS.2020.2965188

Spin-Coater Machine Control via Passivity With Sliding Modes

HÉCTOR HUERTA[1] AND NIMROD VÁZQUEZ[2], (Senior Member, IEEE)
[1]Centro Universitario de los Valles, Universidad de Guadalajara, Ameca 46600, México
[2]Department of Electronics, Technological Institute of Celaya, Celaya 38010, México

Corresponding author: Héctor Huerta (hector.huerta@profesores.valles.udg.mx)

This work was supported by the División de Estudios Científicos y Tecnológicos, Centro Universitario de los Valles, Universidad de Guadalajara.

ABSTRACT In this paper, a novel control scheme for a spin-coater machine is presented, based on Passivity and Sliding Modes. The machine is used to make semiconductor thin films with a centrifugation force. A brushless direct current motor was selected as an actuator, its mathematical model is presented, including the mechanical and electrical dynamics. The control objective is the rotor speed regulation, with maximum acceleration. Taking advantage of the energy properties of the system, a sliding manifold is selected and, in order to reject the matched perturbations, the Integral Sliding Modes technique is applied. Then, with the unperturbed system, a passivity feedback is applied, to guarantee the stability around the desired equilibrium point. To complete the control scheme, an observer is included to estimate the unmeasurable estates. To prove the effectiveness of the proposed control scheme, it was implemented in a spin-coater machine and compared with a gain scheduled PID. The experimental results show a good performance of the closed-loop system, in spite of perturbations.

INDEX TERMS Brushless motors, nonlinear control systems, sliding mode control, spinning machines.

I. INTRODUCTION

In the synthesis and development of thin films with new materials there are some procedures used in a laboratory. One of the most important methods is the spin-coating technique, which is used to apply thin and uniform films on flat substrates, in general glass sheets. This procedure consists of four stages: 1) Deposit, 2) spin up, 3) spin off, and 4) evaporation. The first three steps must be carried out sequentially, and the fourth occurs during the first three stages, and corresponds to the main mechanism in the thinning of the film. In the deposit step, an amount of substance, containing a new material mixed with solvent, is supplied on the center of a substrate. According to the spin-coater user needs, the substrate could have different dimensions, it is placed and held on a spinning disk and is maintained by using a tape or a vacuum pump, where the last suction method is preferred because it is safer. An excess in the solution is supplied to avoid inconsistencies in the film and the total evaporation of the solvent before reach the desired thickness [1].

The associate editor coordinating the review of this manuscript and approving it for publication was Ning Sun.

In the first stage, the substrate could stay static or spinning with low speed, typically 500 RPM. The second step corresponds to spin up, where the angular speed is incremented. Depending on the desired thickness and applied solution, the angular speed could be as high as 10,000 RPM, and must be controlled with high precision, without variations, to guarantee the film quality and achieve repeatability in the results. In the second step, the substrate is totally covered with the deposited material. The angular speed provokes that the exceeded material can be eliminated by means of the centrifugal force. Once the desired angular speed is reached, the spin off step starts. In the third step, the user selects the time in which the substrate will be rotating at the steady-state speed that depends on the material density and desired thickness. According to the material properties, several spin up and spin off steps could be required by the user. The evaporation step occurs during the entire process, since the deposit step. The fourth step is concluded with a thermal treatment to retire the excess of solvent. Then, the spin-coater machine must have the flexibility to be programmed with several speed increments, with different time in every selection and high precision. The angular speed must have a wide range, starting at low speed and reaching high speed,

which is required by the procedure, in this case it can reach up to 10,000 RPM. Moreover, substrates with a considerable variety of dimensions must be installed in a secure way [1].

In [2] a low cost spin coater machine is presented, where a brushed DC motor was used. However, the use of this actuator has some disadvantages, for example, it could not be applied for a wide range of thin films because of its limited speed range. Moreover, the number of spin up and spin off steps are limited to one, and the open loop controller does not offer robustness under perturbations. In [3], a closed-loop controller for a spin-coater machine was presented, but the substrate angular speed range is limited due to the use of a brushed DC motor. An AC motor was implemented in [4], but the speed range is limited again.

To avoid the disadvantages of the brushed DC motors, a Brushless DC Motor (BLDC) could be used [5], [6]. In [7], [8], the BLDC was applied in spin coater machines with classical linear controllers. Moreover, the entire BLDC operation region corresponds to a nonlinear manifold. Then, the application of linear controllers over a wide range of the angular speed could not guarantee stability of the system and/or satisfactory performance of the closed loop system, because the controller is tuned around a neighborhood of a single equilibrium point [9]. Moreover, these machines are limited to a single spin up and spin off steps, which could reduce the flexibility.

In order to avoid the disadvantages of the linear controller with a fixed gain, the Gain Scheduling technique can be applied, dividing a complete nonlinear region in small linear regions [10]. Gain scheduling technique has been applied in electromechanical systems, however, the tuning could be difficult due to it is necessary to adjust several parameters [11]. Furthermore, nonlinear control techniques could be applied to the BLDC motor, including adaptive control [12], intelligent control [13], [14], backstepping [15] and other techniques like torque control [16]. However, the controllers presented were implemented in several applications, different from the spin-coater machines, which need different requirements and are subject to different conditions.

Additionally, sliding modes (SM) control technique offers robustness against parameter variations and external disturbances, which can be done with fast response [17]. This methodology can be applied to linear and nonlinear systems, and consists of two parts. The first part is to design a sliding manifold in which the closed-loop system has the desired properties. In the second part a discontinuous control law is selected to enforce the trajectories of the system to converge to the sliding manifold. If the manifold is designed as a function of the nonlinear operation region, it is possible to cope the nonlinear behavior of the system [18]. Sliding mode controllers have been applied in electrical machines [19]–[23]. In particular, a controller based on sliding modes for electric power systems was presented in [24], taking into account a passivity model. Although the electrical machine in [24] corresponds to a synchronous machine, as in this work, the dynamical behavior is different and lacks of experimental results. Moreover, in [25] the sliding modes control technique was applied to a spin-coater machine, however, the block control technique was used in the sliding manifold design, which cause the cancellation of some nonlinear terms that could contribute to the system stability.

In this paper a spin-coater machine to make thin films is presented. The mechanical stage is composed by a spinning disk to attach a substrate from 1'' to 5'' with a vacuum pump, a transparent cover, a mobile arm to hold the solution dispenser and a housing to install the components. A BLDC was selected as the actuator, due to the high-speed range. The electronic stage is composed of a three-phase power inverter, with a discrete time control scheme, embedded in a microprocessor with Advanced RISC Machine (ARM) architecture. Moreover, a user Human Machine Interface (HMI), including a matrix keyboard and an LCD is considered. The embedded algorithm enables to configure until three spin up and three spin off steps with different steady-state speed and time. This combination enables to cope with the nonlinear operation region of the BLDC from 500 RPM to 10,000 RPM, and presents some advantages over the commercial spin coater machines. The main contribution of this paper is a novel control scheme, including a state observer, considering the passivity approach [26] and the integral SM control [18], taking into account the spin-coater machine designed and implemented. In order to guarantee a high performance in the thin films making, the complete dynamics of the BLDC machine are described by a seventh order mathematical model. The control objective is the regulation of the rotor speed with the maximum acceleration. A positive definite Hamiltonian function is formulated as the sum of the mechanical and electrical energies, and the BLDC dynamics are presented in the Hamilton form. A nonlinear sliding manifold is formulated, taking into account the passivity approach, where the speed control error tends to zero. The former approach is able to avoid the elimination of the electrical torque terms, as in some feedback linearization techniques, to obtain the system stability. Moreover, the integral SM technique guarantees robustness of the closed-loop system with respect to the matched uncertainties [18]. Combining integral SM and passivity approaches it is possible to stabilize the closed-loop system and, moreover, to reject the unknown and bounded matched perturbations, which enables a high performance of the spin coater machine, to make a high quality thin films, with a high angular speed range and flexibility. Finally, the unmeasurable estates of the system are estimated by an observer. To show the effectiveness of the proposed control scheme, it was implemented in the developed spin-coater machine, with an embedded system composed by a 32 bits ARM microcontroller. Furthermore, a gain scheduling PID controller is implemented, to compare the performance of the proposed controller and show the advantages in the closed-loop system.

The rest of the paper is organized as follows. In *Section II* some important issues in the implementation of a spin-coater machine are introduced. *Section III* presents the mathematical

FIGURE 1. Motor housing with spinning disk.

model of the system. *Section IV* shows the development of the proposed Passivity with Sliding Modes control technique and, then, in *Section V* it is applied to the spin-coater machine. In *Section VI*, a gain scheduled PID is designed. The experimental results are presented in *Section VII*, followed by conclusion, in *Section VIII*.

II. SPIN-COATER DEVELOPMENT

The spin-coater machine development includes the mechanical stage, electronic stage and embedded control scheme. In this section the mechanical and electronic stages are presented. Then, in *Section V,* the proposed passivity with sliding modes control algorithm is presented.

A. MECHANICAL STAGE

In this stage, the BLDC mounting structure, spinning disk, housing and protective cover are presented. The BLDC mounting was made of aluminum 6061, due to its mechanical properties and availability. The spinning disk has five concentric circumferences with diameters from 1'' to 5'' and it was made of aluminum 6061, which was selected by the low weight that reduces the mechanical torque in the BLDC motor. In order to cope with substrates with several sizes and forms, five diameters are included in the disk. The substrate must cover completely a circle with the proper diameter. An o-ring is installed in a circumference, depending on the substrate size, to hold the disk when the vacuum pump starts, avoiding air leaks. In Fig. 1, the BLDC motor housing with the spinning disk is presented.

Taking into account the mechanical design, a rotary actuator was selected. Based on the computed mechanical requirements, that is, the angular speed, angular acceleration and inertia constant, it follows

$$T_m = 48\ mNm,$$
$$P = 50.2656\ W,$$

TABLE 1. Maxon 449464 bldc parameters.

Nominal voltage	24V
No load speed	13,200 RPM
No load current	280mA
Nominal speed	10,200 RPM
Nominal torque	52.7mNm
Nominal current	2.79A
Stall torque	773mNm
Stall current	45.8[a]
Max. efficiency	85%

where T_m is the mechanical torque and P is the required power at 10,000 RPM. Then, the selected actuator was the three phase Maxon BLDC 449464, the parameters are shown in Table 1.

B. ELECTRONIC STAGE

The electronic stage consists on the power stage, and control stage. In the case of the power stage, the BLDC motor is a three phase synchronous machine with a permanent magnet rotor. As a consequence, there are some rotating magnetic fields in the rotor with the commutation functions in the stator [27]. The rotor speed can be measured through Hall sensors, located inside the motor housing. The selected Maxon 449464 BLDC has three Hall effect sensors and the rotor has seven pole pairs, so, there are seven pulses in every sensor per revolution. The output resulting from the sensors corresponds to a sequence of six states that represents the relative rotor position. The electronic power stage consists of three branches with power MOSFETs, every branch supply the voltage to a BLDC phase [27]. The commutation signals required are generated in the electronic control stage, by the speed controller. The proposed control scheme, as well as a gain scheduled PID, was implemented in an electronic embedded system based on a 32 bits microcontroller Atmel SAM3X8E, ARM Cortex – M3 CPU. The proposed control scheme requires the speed estimation, which is compared with the reference speed. The reference speed is defined by the user, there are until three different steps of speed, with different period. These parameters are introduced through the user interface, composed of a matrix keypad and a liquid crystal display. The rotor speed is estimated in the microcontroller, considering the square signal provided by the Hall sensors, which are inside the BLDC. With the previous characteristics of the spin-coater, the proposed nonlinear robust control scheme via passivity with integral sliding modes was developed. In addition, a gain scheduled PID was designed to compare the performance of the proposed control scheme. The results obtained are shown in the next sections.

III. PLANT MODEL

In order to develop the mathematical model of the BLDC, consider that the machine is a symmetrical and balanced

system and the mechanical torque input, T_m, can be defined as a constant function of time, that is $\dot{T}_m = 0$.

A. BLDC MODEL

After the Park's transformation and considering the Kirchhoff and Faraday laws, the electrical equilibrium equations of a BLDC can be written in a matrix form as follows [27]

$$\boldsymbol{v}_{dq} = \boldsymbol{R}_{dq}\boldsymbol{i}_{dq} + \frac{d}{dt}\boldsymbol{\lambda}_{dq} + \boldsymbol{A}_{\omega}\boldsymbol{\lambda}_{dq}, \tag{1}$$

where $\boldsymbol{v}_{dq} = \left[v_f 000 v_d v_q\right]^T$, v_f, is the field voltage , v_d and v_q are the stator direct and quadrature axis voltages, respectively; $\boldsymbol{i}_{dq} = [\boldsymbol{i}_r \boldsymbol{i}_s]^T$, $\boldsymbol{i}_r = \left[i_f i_g i_{kd} i_{kq}\right]^T$, $\boldsymbol{i}_s = \left[i_d i_q\right]^T$, i_f is the field current, i_g, i_{kd} and i_{kq} are the rotor damping windings currents, i_d and i_q are the stator direct and quadrature axis currents; $\boldsymbol{\lambda}_{dq} = [\boldsymbol{\lambda}_r \boldsymbol{\lambda}_s]^T$, $\boldsymbol{\lambda}_r = \left[\lambda_f \lambda_g \lambda_{kd} \lambda_{kq}\right]^T$, $\boldsymbol{\lambda}_s = \left[\lambda_d \lambda_q\right]^T$, λ_f is the field flux, λ_g, λ_{kd} and λ_{kq} are the rotor damping windings flux linkages, λ_d and λ_q are the stator direct and quadrature axis flux linkages; $\boldsymbol{R}_{dq} = diag\left\{r_f r_g r_{kd} r_{kq} r_s r_s\right\}$, r_f is the field resistance; r_g, r_{kd} and r_{kq} are the rotor damping windings resistances, r_s is the stator resistance and $\boldsymbol{A}_{\omega} = \begin{bmatrix} 0 & 0 \\ 0 & \boldsymbol{I}(\omega) \end{bmatrix}$, $\boldsymbol{I}(\omega) = \begin{bmatrix} 0 & -\omega \\ \omega & 0 \end{bmatrix}$.

In addition, the flux linkages vector $\boldsymbol{\lambda}_{dq}$ is defined as

$$\boldsymbol{\lambda}_{dq} = \boldsymbol{L}_{dq}\boldsymbol{i}_{dq}, \tag{2}$$

where $\boldsymbol{L}_{dq} = \begin{bmatrix} \boldsymbol{L}_{11} & -\boldsymbol{L}_{12} \\ \boldsymbol{L}_{12}^T & \boldsymbol{L}_{22} \end{bmatrix}$, $\boldsymbol{L}_{22} = \begin{bmatrix} -L_d & 0 \\ 0 & -L_q \end{bmatrix}$, $\boldsymbol{L}_{11} = \begin{bmatrix} L_f & 0 & L_{md} & 0 \\ 0 & L_g & 0 & L_{mq} \\ L_{md} & 0 & L_{kd} & 0 \\ 0 & L_{mq} & 0 & L_{kq} \end{bmatrix}$ and $\boldsymbol{L}_{12} = \begin{bmatrix} L_{md} & 0 \\ 0 & L_{mq} \\ L_{md} & 0 \\ 0 & L_{mq} \end{bmatrix}$.

Furthermore, L_d and L_q are the stator direct and quadrature inductances, respectively; L_f is the field inductance, L_g, L_{kd} and L_{kq} are the rotor windings inductances; L_{md} and L_{mq} are the direct and quadrature magnetization inductances, respectively.

Then, taking into account (1) and (2) the flux linkages, $\boldsymbol{\lambda}_{dq}$, dynamics can be rewritten as follows

$$\frac{d}{dt}\boldsymbol{\lambda}_{dq} = -\left[\boldsymbol{R}\boldsymbol{L}_{dq}^{-1} + \boldsymbol{A}_{\omega}\right]\boldsymbol{\lambda}_{dq} + \boldsymbol{v}_{dq}. \tag{3}$$

The mechanical dynamics for the BLDC are governed by [27]

$$\frac{d\omega}{dt} = \frac{1}{2J_m}\left(T_m - T_e - b_m\omega\right), \tag{4}$$

where ω and ω_b are the rotor speed and the synchronous speed, respectively, J_m is the inertia constant, b_m is the friction constant and T_e is the electromechanical torque, which can be expressed as a function of the stator linked fluxes and stator currents, as follows:

$$T_e = \lambda_q i_d - \lambda_d i_q. \tag{5}$$

In the next subsection an additional representation is introduced, based on the Hamiltonian function.

B. PASSIVITY BASED MODEL

Based on the energy properties of the BLDC, a Hamiltonian mathematical representation of the model (1) - (5) is presented. Considering the increment of the energy around and equilibrium point of the BLDC, the Hamiltonian function can be expressed as follows [26], [28]

$$H = H_m + H_e, \tag{6}$$

where H_m is the mechanical energy and H_e is the electrical energy. The mechanical energy can be presented as a quadratic function of the rotor speed:

$$H_m = \frac{1}{2J_m}\left[J_m\left(\omega - \omega_b\right)\right]^2. \tag{7}$$

Furthermore, the electrical energy can be expressed as quadratic form of the rotor fluxes, that is,

$$H_e = \frac{1}{2}\left(\boldsymbol{\lambda}_{dq} - \boldsymbol{\lambda}_{dq,ss}\right)^T \boldsymbol{L}_{dq}^{-1}\left(\boldsymbol{\lambda}_{dq} - \boldsymbol{\lambda}_{dq,ss}\right), \tag{8}$$

where $\boldsymbol{\lambda}_{dq,ss}$ is the steady-state vector for $\boldsymbol{\lambda}_{dq}$. The, from (7) and (8), the energy function (6) is defined as

$$H = \frac{1}{2}\boldsymbol{x}^T\boldsymbol{A}_H^{-1}\boldsymbol{x}, \tag{9}$$

with $\boldsymbol{A}_{Hi} = \begin{bmatrix} J_{mi} & 0 \\ 0 & \boldsymbol{L}_{dqi} \end{bmatrix}$ and $\boldsymbol{x}$ as the state vector:

$$\boldsymbol{x} = \begin{bmatrix} x_1 \\ x_2 \\ x_3 \\ x_4 \\ x_5 \\ x_6 \\ x_7 \end{bmatrix} = \begin{bmatrix} J_m\left(\omega - \omega_b\right) \\ \lambda_f - \lambda_{f,ss} \\ \lambda_g - \lambda_{g,ss} \\ \lambda_{kd} - \lambda_{kd,ss} \\ \lambda_{kq} - \lambda_{kq,ss} \\ \lambda_d - \lambda_{d,ss} \\ \lambda_q - \lambda_{q,ss} \end{bmatrix}. \tag{10}$$

Then, from (2), (4) and (6)-(10) the Hamiltonian BLDC model is finally written as [28]

$$\dot{x} = \left[\boldsymbol{J}(\boldsymbol{x}) - \boldsymbol{R}\right]\frac{\partial H(\boldsymbol{x})}{\partial \boldsymbol{x}} + \boldsymbol{b}u + \boldsymbol{g}(\boldsymbol{x}, t), \tag{11}$$

where $\boldsymbol{b} = [0\,1\,0\,0\,0\,0\,0]^T$, $u = v_f - v_{f,ss}$ is the control input, $v_{f,ss}$ is the excitation voltage around the equilibrium point, $\boldsymbol{J}(\boldsymbol{x})$ is a skew-symmetric matrix that is composed by the state interconnections:

$$\boldsymbol{J}(\boldsymbol{x}) = \begin{bmatrix} 0_{1\times 5} & \lambda_q & -\lambda_d \\ & 0_{4\times 7} & \\ -\lambda_q & & 0_{1\times 6} \\ \lambda_d & & 0_{1\times 6} \end{bmatrix},$$

$\boldsymbol{R}$ is a positive definite matrix, which contains the dissipative terms:

$$\boldsymbol{R} = \text{diag}\left\{b_m r_f r_g r_{kd} r_{kq} r_s r_s\right\},$$

and $\boldsymbol{g}(\boldsymbol{x}, t)$ is a vector that includes the perturbation terms, e.g., parameter variations and external disturbances due to

changes in the electrical network. In this case, the perturbations can be written as variations in the excitation current, that is:

$$\boldsymbol{g} = \left[0\ \alpha\ r_f i_f 0\ 0\ 0\ 0\ 0\right]^T, \quad \alpha \in \mathbb{R}.$$

Furthermore, from (6) - (9), and taking into account that $\boldsymbol{i}_{dq} = d/dt\boldsymbol{\lambda}_{dq}$ [26], the derivative $\partial H(\boldsymbol{x})/\partial \boldsymbol{x}$ of (10) can be calculated as

$$\frac{\partial H(\boldsymbol{x})}{\partial \boldsymbol{x}} = \begin{bmatrix} \omega - \omega_b \\ \boldsymbol{i}_{dq} - \boldsymbol{i}_{dq,ss} \end{bmatrix}, \tag{12}$$

which leads to the passive output

$$y(\boldsymbol{x}) = \boldsymbol{b}\frac{\partial H(\boldsymbol{x})}{\partial \boldsymbol{x}} = i_f - i_{f,ss}. \tag{13}$$

The increment of the field current $i_f - i_{f,ss}$ in (13) can be found by using (2) and computed as a function of the increment in the fluxes:

$$\boldsymbol{i}_{dq} - \boldsymbol{i}_{dq,ss} = \boldsymbol{L}_{dq}^{-1}\left(\boldsymbol{\lambda}_{dq} - \boldsymbol{\lambda}_{dq,ss}\right).$$

IV. PASSIVITY WITH SLIDING MODES CONTROL

The passivity with sliding modes approach is described in this section. At first, the passivity property is introduced [26]:

Definition 1: Given the supply rate $\boldsymbol{r}(\boldsymbol{x}) = u^T y(\boldsymbol{x})$, a system is passive with respect to the output $y(\boldsymbol{x})$ if there exists a continuous differentially function $H(\boldsymbol{x})$, called storage function, such that

$$H(\boldsymbol{x}) \leq H(\boldsymbol{x}_0) + \int_{t_0}^{t_1} \boldsymbol{r}(s)\, ds. \tag{14}$$

Consider the class of nonlinear systems that can be presented in the Hamiltonian form with dissipative terms [26], as in the BLDC system (11), i. e.

$$\begin{aligned} \dot{x} &= \left[\boldsymbol{J}(\boldsymbol{x}) - \boldsymbol{R}(\boldsymbol{x})\right]\frac{\partial H(\boldsymbol{x})}{\partial \boldsymbol{x}} + \boldsymbol{b}(\boldsymbol{x})\, u + \boldsymbol{g}(\boldsymbol{x}, t) \\ y &= \boldsymbol{b}(\boldsymbol{x})\frac{\partial H(\boldsymbol{x})}{\partial \boldsymbol{x}}, \end{aligned} \tag{15}$$

where $\boldsymbol{x} \in R^n$ is the state vector, $u \in R$ is the control input, $y(\boldsymbol{x}) \in R$ is the output, $\boldsymbol{g}(\boldsymbol{x}, t)$ is the perturbation term, which includes parameter variations and external disturbances, $H(\boldsymbol{x})$ is the Hamiltonian function that represents the increment of the energy around an equilibrium point, $\boldsymbol{J}(\boldsymbol{x})$, is a skew-symmetric matrix, which includes the states interconnections and $\boldsymbol{R}(\boldsymbol{x})$, which contains the dissipative terms, is a symmetric positive-definite matrix. In the case of the unperturbed system, i. e., with $\boldsymbol{g}(\boldsymbol{x}, t) = 0$ in (15), if the Hamiltonian energy function $H(\boldsymbol{x})$ corresponds to a positive definite function, the passive output feedback

$$u = -k_0 y(\boldsymbol{x}), \quad k_0 > 0, \tag{16}$$

is able to stabilize the system around the origin, $\boldsymbol{x} = 0$ [26]. However, when the perturbations are presented, as in (15), the control law (16) lacks of robustness. Therefore, in this paper, to add robustness to the control law (16), the integral sliding modes is proposed, to develop the Passivity with Sliding Modes (PSM) technique.

Consider the following assumptions:

H1. The Hamiltonian (14) is a positive definite function.

H2. The BLDC nominal parameters of the pin-coater are known.

H3. The perturbation term $\boldsymbol{g}_i(\boldsymbol{x}_i, t)$ in (15) fulfils the matching condition, such that there exists a function $\bar{g}(\boldsymbol{x}, t)$, which satisfies

$$\boldsymbol{g}(\boldsymbol{x}, t) = \boldsymbol{b}(\boldsymbol{x})\,\bar{g}(\boldsymbol{x}, t), \quad \bar{g}(\boldsymbol{x}, t) \in \mathbb{R}. \tag{17}$$

Under *Assumptions H.1 – H.3*, the BLDC control scheme is proposed, to add robustness with the respect to the matched perturbation term $\boldsymbol{g}_i(\boldsymbol{x}_i, t)$.

According to the Integral Sliding Modes (ISM) technique [18], to reject the perturbation term $\boldsymbol{g}_i(\boldsymbol{x}_i, t)$ in (15), the control input u in (1) is redefined as

$$u = u_0 + u_1, \tag{18}$$

where the second part, u_1, is chosen to reject the perturbation term $\boldsymbol{g}(\boldsymbol{x}, t)$ and the first part, u_0, is selected to stabilize the system (15), A sliding manifold is designed as

$$s(\boldsymbol{x}) = H(\boldsymbol{x}) + \sigma(t) = 0, \quad s \in R, \tag{19}$$

with $\sigma \in R$ as an integral vector. From (15) and (17), the sliding mode motion on the manifold (19) can be written as:

$$\begin{aligned} \dot{s}(\boldsymbol{x}, t) = &\left(\frac{\partial H(\boldsymbol{x})}{\partial \boldsymbol{x}}\right)^T \left[\left[\boldsymbol{J}(\boldsymbol{x}) - \boldsymbol{R}(\boldsymbol{x})\right]\frac{\partial H(\boldsymbol{x})}{\partial \boldsymbol{x}} + \boldsymbol{b}(\boldsymbol{x})\, u_0\right] \\ &+ \left(\frac{\partial H(\boldsymbol{x})}{\partial \boldsymbol{x}}\right)^T \boldsymbol{b}(\boldsymbol{x})\left[u_1 + \bar{g}(\boldsymbol{x}, t)\right] + \dot{\sigma}(\boldsymbol{x}), \end{aligned} \tag{20}$$

where the dynamics for $\dot{\sigma}(t)$ are selected to eliminate the nominal terms in (20), that is

$$\begin{aligned} \dot{\sigma}(t) &= -\left(\frac{\partial H(\boldsymbol{x})}{\partial \boldsymbol{x}}\right)^T \left[\left[\boldsymbol{J}(\boldsymbol{x}) - \boldsymbol{R}(\boldsymbol{x})\right]\frac{\partial H(\boldsymbol{x})}{\partial \boldsymbol{x}} + \boldsymbol{b}(\boldsymbol{x})\, u_0\right], \\ \sigma(0) &= -H(\boldsymbol{x}(0)) \end{aligned} \tag{21}$$

Then, the equation (20) becomes

$$\dot{s}(\boldsymbol{x}, t) = \left(\frac{\partial H(\boldsymbol{x})}{\partial \boldsymbol{x}}\right)^T \boldsymbol{b}(\boldsymbol{x})\left[u_1 + \bar{g}(\boldsymbol{x}, t)\right]. \tag{22}$$

The second part of (18), u_1, is chosen as

$$u_1 = -k_1 sign\left(s(\boldsymbol{x}, t)\right), \quad k_1 > 0. \tag{23}$$

Thus, under the condition

$$k_1 > \left|\bar{g}(\boldsymbol{x}, t)\right|,$$

a SM motion is achieved on the manifold $s(\boldsymbol{x}, t) = 0$, (19), since $t = 0$ that is presented as

$$\dot{x} = \left[\boldsymbol{J}(\boldsymbol{x}) - \boldsymbol{R}(\boldsymbol{x})\right]\frac{\partial H(\boldsymbol{x})}{\partial \boldsymbol{x}} + \boldsymbol{b}(\boldsymbol{x})\left[u_{1,eq} + \bar{g}(\boldsymbol{x}, t) + u_0\right], \tag{24}$$

with $u_{1,eq}$ as the equivalent control computed from $\dot{s}(\boldsymbol{x}, t) = 0$, (22), i. e.,

$$u_{1,eq} = -\bar{g}(\boldsymbol{x}, t).$$

Then, the equivalent control, $u_{1,eq}$, rejects the perturbation term in (24) since $t = 0$ [18]. Therefore, the equation (15) reduces to the unperturbed system:

$$\dot{x} = [\boldsymbol{J}(\boldsymbol{x}) - \boldsymbol{R}(\boldsymbol{x})] \frac{\partial H(\boldsymbol{x})}{\partial \boldsymbol{x}} + \boldsymbol{b}(\boldsymbol{x}) u_0$$
$$y = \boldsymbol{b}(\boldsymbol{x}) \frac{\partial H(\boldsymbol{x})}{\partial \boldsymbol{x}}, \tag{25}$$

Finally, the first part of the control input (18), u_0, in (25) is chosen as a classical passive output feedback, as in (16).

Now, the following result can be established:

Theorem 1: If the *Assumptions H.1 - H.3* holds, the solution of the closed-loop system (15) with (18) tends asymptotically to its steady-state value.

Proof.

Based on the previous procedure, choose the second part of (18), u_1, as in (23), with (19) and (21). Under the *Assumption H.3*, and the condition

$$k_1 > |\bar{g}(\boldsymbol{x}, t)|$$

the equivalent control, calculated as

$$u_{1,eq} = -\bar{g}(\boldsymbol{x}, t),$$

compensates exactly the perturbation term $\boldsymbol{g}(\boldsymbol{x}, t)$ in (15) since the first instant of time, $t = 0$ [18]. Then, the system (15) becomes to the unperturbed system (25).

On the other hand, considering the first part of (18), u_0, in (25), as

$$u_0 = -k_0 y(\boldsymbol{x}), \quad k_0 > 0, \tag{26}$$

the closed-loop system stability can be achieved by using the Lyapunov function

$$V = H(\boldsymbol{x}). \tag{27}$$

Taking into account the power balance [26]

$$\frac{dH(\boldsymbol{x})}{dt} = -\frac{\partial H(\boldsymbol{x})}{\partial \boldsymbol{x}} \boldsymbol{R}(\boldsymbol{x}) \left(\frac{\partial H(\boldsymbol{x})}{\partial \boldsymbol{x}}\right)^T + u y(\boldsymbol{x}), \tag{28}$$

where

$$\frac{\partial H(\boldsymbol{x})}{\partial \boldsymbol{x}} \boldsymbol{R}(\boldsymbol{x}) \frac{\partial H(\boldsymbol{x})}{\partial \boldsymbol{x}}^T$$

represents the energy dissipation due to the resistive elements. Then, considering (26), it follows:

$$\frac{dH(\boldsymbol{x})}{dt} = -\frac{\partial H(\boldsymbol{x})}{\partial \boldsymbol{x}} \boldsymbol{R}(\boldsymbol{x}) \left(\frac{\partial H(\boldsymbol{x})}{\partial \boldsymbol{x}}\right)^T - k_0 y^2(\boldsymbol{x}). \tag{29}$$

Finally, under the *Assumption H.1*, the derivative (29) is negative definite and, thus, the solution of the closed-loop system (15) with (18) tends asymptotically to zero.

V. SPIN COATER CONTROL

Now, the previous result will be applied to the BLDC in the spin-coater machine, to consider the control objective, that is, the spinning disk speed regulation. Moreover, to complete the control scheme an observer is included to estimate the unmeasurable estates, i. e., the increment around the equilibrium point of the rotor fluxes.

A. SPEED CONTROL

Following the procedure defined in the *Section IV*, the control law u in (11) is redefined as

$$u = u_0 + u_1, \tag{30}$$

where the first part u_0 is selected to stabilize the rotor speed and the second part, u_1, is chosen to reject the perturbation vector $\boldsymbol{g}(\boldsymbol{x}, t)$ in (11). Now, to propose the second part of (30), an integral SM sliding variable s is defined as

$$s = H(\boldsymbol{x}) + \sigma = 0. \tag{31}$$

From (31) and, under the *Assumption H.3*, it follows

$$\dot{s} = \frac{\partial H(\boldsymbol{x})}{\partial \boldsymbol{x}}^T \left[[\boldsymbol{J}(\boldsymbol{x}) - \boldsymbol{R}(\boldsymbol{x})] \frac{\partial H(\boldsymbol{x})}{\partial \boldsymbol{x}} + \boldsymbol{b} u_0 \right] + \left(\frac{\partial H(\boldsymbol{x})}{\partial \boldsymbol{x}}\right)^T \boldsymbol{b} [u_1 + \bar{g}(\boldsymbol{x}, t)] + \dot{\sigma}(t), \tag{32}$$

or, equivalently, choosing $\dot{\sigma}(t)$ as in (21) and with $\sigma(0) = -H(\boldsymbol{x}(0))$, it follows

$$\dot{s} = \left(\frac{\partial H(\boldsymbol{x})}{\partial \boldsymbol{x}}\right)^T \boldsymbol{b} [u_1 + \bar{g}(\boldsymbol{x}, t)]. \tag{33}$$

The control input u_1 in (33) can be defined as in (23), i. e,

$$u_1 = -k_1 sign(s(\boldsymbol{x}, t)). \tag{34}$$

Under the condition $k_1 > |\bar{g}(\boldsymbol{x}, t)|$, a sliding mode motion is induced on $s(\boldsymbol{x}, t) = 0$ from $t = 0$. Then, the equivalent control $u_{1,eq} = -\bar{g}(\boldsymbol{x}, t)$, calculated from (33), rejects exactly the perturbation term $\bar{g}(\boldsymbol{x}, t)$, and (11) is reduced to the unperturbed system

$$\dot{x} = [\boldsymbol{J}(\boldsymbol{x}) - \boldsymbol{R}] \frac{\partial H(\boldsymbol{x})}{\partial \boldsymbol{x}} + \boldsymbol{b} u_0. \tag{35}$$

The first part of the control input (35), u_0, is selected as in (16), that is

$$u_0 = -k_0 y(\boldsymbol{x}), \tag{36}$$

where $y(\boldsymbol{x}) = i_f - i_{f,ss}$.

It is important to note that the Hamiltonian function, $H(\boldsymbol{x})$, is presented as a function of the state vector $\boldsymbol{x}$, such that that $H(\boldsymbol{x}) > 0$, for all $\boldsymbol{x} \neq 0$. Moreover, all the nominal parameters of the BLDC are known, from the datasheets of the Maxon 449464 and experimental validation. Then, the *Assumptions H.1* and *H.2* are fulfilled. Thus, from the *Theorem 1*, the solution of the closed – loop system (11) with (30) converges asymptotically to zero.

Remark 1: Regarding the initial condition required by the ISM, that is, $\sigma(0) = -H(\boldsymbol{x}(0))$, for the BLDC in the spin-coater machine, the initial values vector $\boldsymbol{x}(0)$ can be calculated, considering that the mechanical torque is constant and known. Moreover, the speed desired value of the spinning disk is selected by the user. Then, with the computed initial values vector, the SM motion is given since $t = 0$. As a matter of fact, in the general case, the initial values vector $\boldsymbol{x}(0)$ could be difficult to obtain, as a consequence $\sigma(0) \neq -H(\boldsymbol{x}(0))$.

In the spin-coater case, the proposed control scheme (34) enables the closed-loop system trajectories convergence to the manifold (31) in a finite time, [17].

B. STATE OBSERVER

In the previous subsection, the spin-coater speed controller was developed considering that the state vector was available to measurement. However, the rotor fluxes are not available for measurement, then, an observer is required to estimate these variables.

Suppose that the stator voltages, v_{di} and v_{qi}, and rotor speed, ω_i, can be measured. Then, considering (3) and (10), an observer for the spin-coater is presented as follows

$$\dot{\hat{x}}_{dq} = -\left[\boldsymbol{R}\boldsymbol{L}_{dq}^{-1} + \boldsymbol{A}_o\right]\hat{x}_{dq} + \boldsymbol{v}_{dq}, \tag{37}$$

where the vector $\hat{x}_{dq}$ is composed of the estimates of the BLDC fluxes errors, $\hat{x}_{dq} = \left[\hat{x}_2\hat{x}_3\hat{x}_4\hat{x}_5\hat{x}_6\hat{x}_7\right]^T$ and

$$\boldsymbol{A}_o(t) = \begin{bmatrix} 0 & 0 \\ 0 & \boldsymbol{I}_o(t) \end{bmatrix}, \quad \boldsymbol{I}_o(t) = \begin{bmatrix} 0 & -x_1(t) \\ x_1(t) & 0 \end{bmatrix}.$$

In order to analyze the convergence of the observer (37), a linear system with time-varying parameters can be obtained from (3), and (37), which represents the error dynamics, as:

$$\dot{\tilde{x}}_{dq} = -\boldsymbol{R}\boldsymbol{L}_{dq}^{-1}\tilde{x}_{dq} - \boldsymbol{A}_o(t)\tilde{x}_{dq}, \tag{38}$$

where $\tilde{x}_{dq} = \left[\tilde{x}_2\tilde{x}_3\tilde{x}_4\tilde{x}_5\tilde{x}_6\tilde{x}_7\right]^T$, $\tilde{x}_i = x_i - \hat{x}_i$, $i = 2, \ldots 7$.

The eigenvalues of the matrix $\boldsymbol{R}\boldsymbol{L}_{dq}^{-1}$ are real and negative, as a consequence, the matrix is Hurwitz. On the other hand, $\boldsymbol{A}_o(t)$ is a skew-symmetric matrix. Then, the system (38) is asymptotically stable [11].

VI. GAIN SCHEDULED PID CONTROLLER

In order to compare the performance of the proposed control scheme, a linear gain scheduled PID controller was designed. According to [11], the gain scheduling technique can be summarized in the following steps:

1. Divide the entire operation region in some small manifolds, such that every subsystem can be reduced to a linear one.

2. Design a family of parameterized linear controllers for the set of manifolds.

3. Define a gain scheduled controller in such a way that each linear controller stabilizes the system around the equilibrium point without error.

4. Verify the gain scheduled controller performance with the family of local controllers for the complete operation region by means of simulations and experimental results.

Then, with the stated methodology, a gain scheduled PID controller was designed. In the case of step one, considering that the spinning disk requires a minimum speed of 500 RPM and a maximum of 10,000 RPM, six manifolds were defined on the BLDC operation region, which are presented in Table 2. It is important to note that the intersection of the manifolds corresponds to an empty space and the complete operation region is covered completely.

TABLE 2. Gain scheduled controller manifolds.

Manifold	Rotor speed set
m_1	$m_1 = \{\omega \mid 500 \leq \omega > 800\}$
m_2	$m_2 = \{\omega \mid 800 \leq \omega > 1{,}000\}$
m_3	$m_3 = \{\omega \mid 1{,}000 \leq \omega > 1{,}500\}$
m_4	$m_4 = \{\omega \mid 1{,}500 \leq \omega > 2{,}500\}$
m_5	$m_5 = \{\omega \mid 2{,}500 \leq \omega > 5{,}000\}$
m_6	$m_6 = \{\omega \mid 5{,}000 \leq \omega \geq 10{,}000\}$

TABLE 3. Parameters of the scheduled PID.

Manifold	K_p	T_i	T_d
m_1	1.0000	0.0000	2.3160
m_2	0.3000	0.0000	0.0000
m_3	12.0000	4.7840	1.1960
m_4	0.5000	0.0000	0.7098
m_5	1.0000	3.3860	0.0000
m_6	1.0000	0.4930	0.1230

Next, for the step 2, the parameterized family of linear controllers chosen for the BLDC is a classical PID and the control input generated is described by the following expression:

$$u(t) = K_{p,j}e(t) + \frac{K_p}{T_{i,j}}\int_0^t e(\tau)\,d\tau + K_{p,j}T_{d,j}\frac{de(\tau)}{dt}, \tag{39}$$

where $u(t)$ is the BLDC control input, $e(t)$ is the control error given by the difference between the BLDC reference value and measured output, $K_{p,j} \in \mathbb{R}^+$ is the proportional gain, $T_{i,j} \in \mathbb{R}^+$ is the integral time constant, $T_{d,j} \in \mathbb{R}^+$ is the derivative time constant, $j = 1, 2, 3, 4, 5, 6$ represents the corresponding subindex for the j^{th} manifold. Thus, a family of PID controllers can be parameterized by means of the positive constants $K_{p,j}$, $T_{i,j}$ and $T_{d,j}$.

Finally, for the step 3, the scheduled PID parameters for the control scheme are given in Table 3, which were tuned considering a root locus methodology, in the middle point of the corresponding manifold and were adjusted heuristically in the spin coater machine, considering the maximum acceleration.

VII. EXPERIMENTAL RESULTS

In order to prove the effectiveness of the propose control scheme, it was implemented in the spin-coater machine developed. In the figure 2, the schematic diagram applied for the implementation of the closed-loop control scheme given by (30) and (37) is shown. The three phase output terminal voltages (v_a, v_b, v_c) and currents (i_a, i_b, i_c) are measured in the generator, which are sent by the *abc* to *dq0* transformation block, due to the proposed control scheme was developed take into consideration that reference frame. The transformed values v_d, v_q, i_d and i_q are obtained from the state observer and the speed controller. The estimation of the rotor fluxes vector $\hat{\boldsymbol{x}}_{dq}$ is computed by the observer, with the transformed measurements. These values and the rotor speed, measured

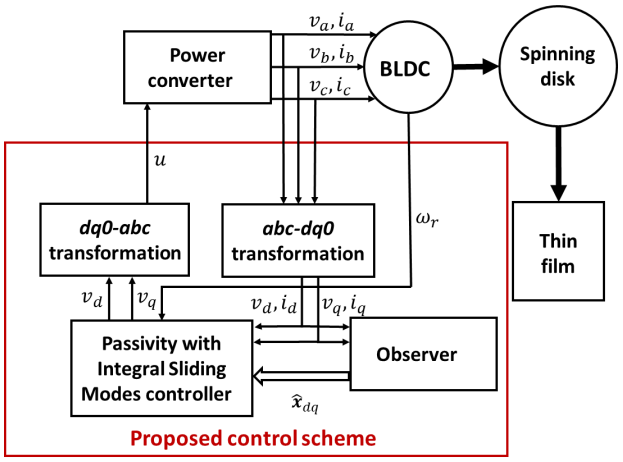

FIGURE 2. Proposed control scheme diagram.

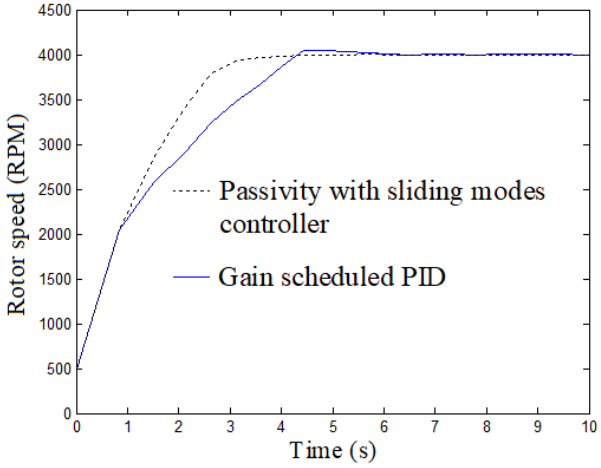

FIGURE 3. Rotor speed response.

directly from the BLDC, are used by the Passivity with Integral Sliding Modes controller, to compute the control signal. Then, the *dq0* to *abc* transformation block is needed to obtain the control input value in the *abc* reference frame. The parameters of the control scheme are computed off-line.

In order to obtain a uniform thickness in the film, the process must have maximum acceleration and regulation of speed, without steady state error, overshoot or oscillations. Then, taking into account those requirements, the parameters of the proposed control scheme were tuned to obtain the minimum stabilization time, without overshoot. The experimental results obtained with an initial value in the speed of 500 RPM and a reference speed value of 4,000 RPM are presented. In order to compare the performance, the responses for the proposed control scheme and the gain scheduled PID are included.

The performance of the closed loop (11) with the proposed control scheme (30) and (37) is presented in figure 3, as well as the response of the gain scheduled PID.

Some important highlights are underlined:

a) The proposed control scheme is able to stabilize the rotor speed around the desired equilibrium point, in this case 4,000 RPM, in 3.2 s, considering a band of 5%. On the other hand, the stabilization time with the gain scheduled PID is 4.3 s. In the process of making films it is important to reduce the stabilization time to achieve the maximum acceleration.

b) The response obtained with the proposed controller corresponds to an overdamped system, without an overshoot. However, the stabilization time is reduced by 1.1 s, compared to the PID. In the case of the gain scheduled PID, an underdamped response is obtained, with an overshoot of 2.5%. As it was mentioned previously, in the making of thin films is better to have an overdamped response, without incrementing the stabilization time, to produce a better result.

c) The proposed control scheme does not present oscillations in steady-state. The gain scheduled PID presents oscillations. It is possible to obtain a homogenous thin film only if oscillations are avoided.

d) The proposed control scheme is able to stabilize the system in the complete nonlinear operation region of the BLDC. Then, it is not necessary to use different controllers in different linear subsystems, as in the gain scheduled PID. In this way, it is easier to tune the parameters of the proposed control scheme.

e) In order to verify the robustness of the proposed controller under parameter variations, the winding stator resistance was reduced 4% and the inertia constant was incremented 3%. The responses with these perturbations are presented in figure 4. The response obtained with the proposed control scheme is the same as in the unperturbed case, which shows the robustness under parameter variations in the closed loop system. On the other hand, with the perturbed system, the response of the gain scheduled PID presents a steady-state error of 3%.

f) Since the BLDC has three windings, the three voltages are supplied through the power converter. The control input to the power converter corresponds to three PWM signals with constant frequency and variable duty cycle. The electronic embedded system generates the corresponding PWM signal, based on the computed duty cycle, provided by the speed controller that are shown in figure 5, for the proposed control scheme and the gain scheduled PID. Again, the proposed controller presents a response without oscillations and overshoot. On the other hand, the gain scheduled PID presents oscillations and overshoot. It is important to note that, at the beginning, both control signals are similar, due to a slow starter for the BLDC was included, to avoid excessive start currents and prevent damages in the electronic components. Moreover, at the begging, both controllers increment the value of the duty cycle until the 100%, to adjust it gradually until the correct value. In the case of the gain scheduled PID, the duty cycle is saturated by 1.9 s, while in the proposed control scheme is 0.6 s, about the 30% compared with the PID. Since it is important to reach the reference speed faster, the parameters of both controllers were tuner to obtain the

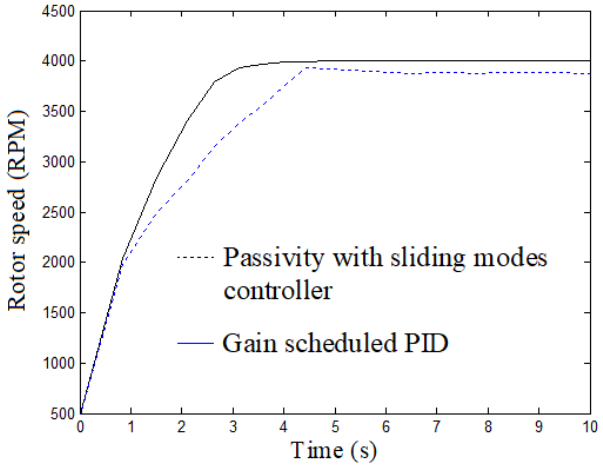

FIGURE 4. Rotor speed response under perturbations.

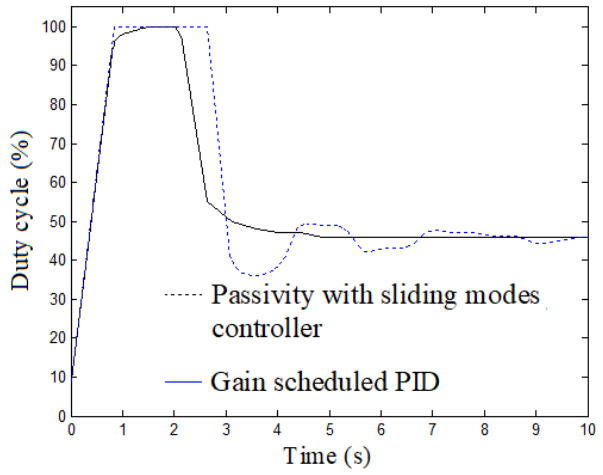

FIGURE 5. Control inputs.

maximum acceleration. The saturation levels are consequences of the gains chosen. However, although there are saturations in the control signals, the control objective is achieved. Moreover, note that the chattering is low, due to the control law (30) is a combination of discontinuous and continuous functions.

It is worth mentioning that several experiments were carried out, considering different equilibrium points, initial speed values and spin off times and a good performance was obtained with the proposed control scheme.

The developed spin coater machine, which includes the Passivity with Sliding Modes closed loop proposed control scheme, was tested to prove its effectiveness in making thin films, in the Laboratory of Environment and Renewable Energy of Centro Universitario de los Valles, Universidad de Guadalajara.

Two examples are presented to prove the effectiveness of the spin-coater machine developed. The results were obtained by using an Atomic Force Microscope (AFM). On the one hand, in the figure 6, is presented a thin film composed of carbon nanotubes and pheophorbides. In this film, a drop of the

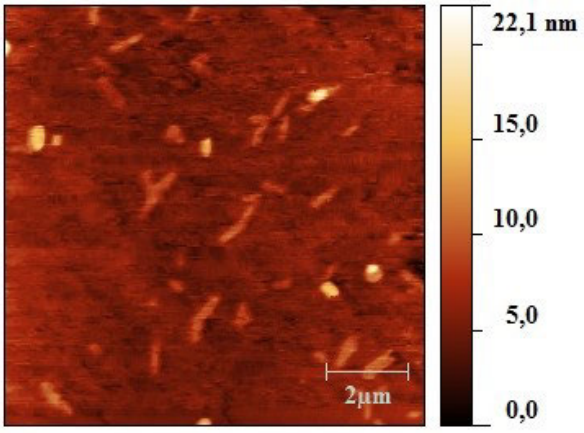

FIGURE 6. Thin films of carbon nanotubes and pheophorbides.

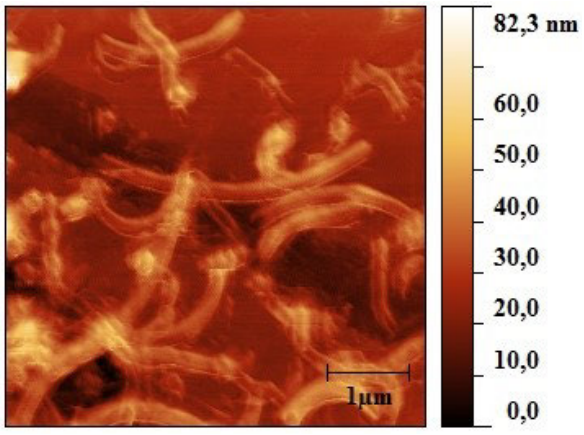

FIGURE 7. Thin films of carbon nanotubes and porphyrins.

substance was supplied to a muscovite mica substrate, which was rotating to 2,500 RPM during 5 s, to produce groups of carbon nanotubes. On the other hand, figure 7 shows a thin film composed of carbon nanotubes and porphyrins. The spin coater machine enables to distribute and fix the carbon nanotubes uniformly. The same technique was applied, i.e., 2,500 RPM during 5 s. The AFM result presents the carbon nanotubes and porphyrins as brilliant points.

VIII. CONCLUSION

A novel robust nonlinear control scheme to a spin-coater machine was developed, with a BLDC motor. The control objective is the rotor speed regulation. The mathematical model includes the electrical and mechanical dynamics. The Hamiltonian model was presented. In order to achieve the rotor speed regulation in the complete nonlinear operation region of the BLDC motor, a Passivity with Sliding Modes technique was applied. At first, based on the Hamiltonian model, the perturbations were rejected, by applying the Integral Sliding Modes technique. Then, a passive feedback was selected to guarantee the closed-loop system stability. Finally, to complete the control scheme, an observer was introduced, to estimate the unmeasurable estates. A compre-

hensive stability analysis of the complete control scheme was presented.

The proposed control scheme, was implemented in a spin-coater machine, to prove the effectiveness. Moreover, the proposed control scheme was compared with a gain scheduled classical PID. The experimental results show a good performance of the proposed Passivity with Sliding Modes controller, since the speed response did not present overshoot and steady state error, with good stabilization time, in spite of perturbations.

ACKNOWLEDGMENT

The authors would like to thank Dr. M. S. Tizapa by his contribution in the development of thin films and the results obtained with the AFM.

REFERENCES

[1] M. Tyona, "A comprehensive study of spin coating as a thin film deposition technique and spin coating equipment," *Adv. Mater. Res.*, vol. 2, no. 4, pp. 181–193, Dec. 2013.

[2] M. Fardousi, M. F. Hossain, M. S. Islam, and S. Rahat, "Cost-effective home-made spin coater for depositing thin films," *J. Mod. Sci. Technol.*, vol. 1, no. 1, pp. 126–134, 2013.

[3] M. F. Hossain, S. Paul, M. A. Raihan, and M. A. G. Khan, "Fabrication of digitalized spin coater for deposition of thin films," in *Proc. Int. Conf. Elect. Eng. Inf. Commun. Technol.*, Apr. 2014, pp. 14–18.

[4] P. Sevvanthi, A. Claude, C. Jayanthi, and A. Poiyamozhi, "Instrumentation for fabricating an indigenous spin coating apparatus and growth of zinc oxide thin films and their characterizations," *Adv. Appl. Sci. Res.*, vol. 3, no. 6, pp. 3573–3580, 2012.

[5] B. Tan, X. Wang, D. Zhao, K. Shen, J. Zhao, and X. Ding, "A lag angle compensation strategy of phase current for high-speed BLDC motors," *IEEE Access*, vol. 7, pp. 9566–9574, 2019.

[6] B. Tian, Q.-T. An, and M. Molinas, "High-frequency injection-based sensorless control for a general five-phase BLDC motor incorporating system delay and phase resistance," *IEEE Access*, vol. 7, pp. 162862–162873, 2019.

[7] R. Bianchi, M. Panssiera, J. Lima, L. Yagura, A. Andrade, and R. Faria, "Spin coater based on brushless DC motor of hard disk drivers," *Prog. Organic Coat.*, vol. 57, no. 1, pp. 33–36, Sep. 2006.

[8] N. Manikandan, "Construction of spin coating machine controlled by arm processor for physical studies of PVA," *Int. J. Electron. Elect. Eng.*, vol. 3, no. 4, pp. 318–322, 2015.

[9] M. S. Rafaq, A. T. Nguyen, H. H. Choi, and J.-W. Jung, "Disturbance rejection of IPMSM drives by simplified Taylor series-based near optimal control scheme in wide speed range," *IEEE Access*, vol. 7, pp. 20553–20566, 2019.

[10] W. A. P. Munoz, A. G. Sellier, and S. G. Castro, "The predictive functional control and the management of constraints in GUANAY II autonomous underwater vehicle actuators," *IEEE Access*, vol. 6, pp. 22353–22367, 2018.

[11] H. Khalil, *Nonlinear Systems*, 3rd ed. Upper Saddle River, NJ, USA: Prentice-Hall, 1996.

[12] H. Melkote and F. Khorrami, "Nonlinear adaptive control of direct-drive brushless DC motors and applications to robotic manipulators," *IEEE/ASME Trans. Mechatronics*, vol. 4, no. 1, pp. 71–81, Mar. 1999.

[13] M. G. Lopez, P. Ponce, L. A. Soriano, A. Molina, and J. J. R. Rivas, "A novel fuzzy-PSO controller for increasing the lifetime in power electronics stage for brushless DC drives," *IEEE Access*, vol. 7, pp. 47841–47855, 2019.

[14] T. L. Kottas, A. D. Karlis, and Y. S. Boutalis, "A novel control algorithm for DC motors supplied by PVs using fuzzy cognitive networks," *IEEE Access*, vol. 6, pp. 24866–24876, 2018.

[15] L. Sheng, G. Xiaojie, and Z. Lanyong, "Robust adaptive backstepping sliding mode control for six-phase permanent magnet synchronous motor using recurrent wavelet fuzzy neural network," *IEEE Access*, vol. 5, pp. 14502–14515, 2017.

[16] Q. Zhang, J. Deng, and N. Fu, "Minimum copper loss direct torque control of brushless DC motor drive in electric and hybrid electric vehicles," *IEEE Access*, vol. 7, pp. 113264–113271, 2019.

[17] Z. Li, S. Zhou, Y. Xiao, and L. Wang, "Sensorless vector control of permanent magnet synchronous linear motor based on self-adaptive super-twisting sliding mode controller," *IEEE Access*, vol. 7, pp. 44998–45011, 2019.

[18] V. I. Utkin, J. Guldner, and J. Shi, *Sliding Mode Control in Electro-Mechanical Systems*. London, U.K.: Taylor & Francis, 1999.

[19] E.-K. Kim, J. Kim, H. T. Nguyen, H. H. Choi, and J.-W. Jung, "Compensation of parameter uncertainty using an adaptive sliding mode control strategy for an interior permanent magnet synchronous motor drive," *IEEE Access*, vol. 7, pp. 11913–11923, 2019.

[20] F. M. Zaihidee, S. Mekhilef, and M. Mubin, "Application of fractional order sliding mode control for speed control of permanent magnet synchronous motor," *IEEE Access*, vol. 7, pp. 101765–101774, 2019.

[21] E. Lu, W. Li, X. Yang, and S. Xu, "Composite sliding mode control of a permanent magnet direct-driven system for a mining scraper conveyor," *IEEE Access*, vol. 5, pp. 22399–22408, 2017.

[22] A. T. Woldegiorgis, X. Ge, S. Li, and M. Hassan, "Extended sliding mode disturbance observer-based sensorless control of IPMSM for medium and high-speed range considering railway application," *IEEE Access*, vol. 7, pp. 175302–175312, 2019.

[23] X. Liu, H. Yu, J. Yu, and Y. Zhao, "A novel speed control method based on port-controlled Hamiltonian and disturbance observer for PMSM drives," *IEEE Access*, vol. 7, pp. 111115–111123, 2019.

[24] H. Huerta, A. G. Loukianov, and J. M. Canedo, "Passivity sliding mode control of large-scale power systems," *IEEE Trans. Control Syst. Technol.*, vol. 27, no. 3, pp. 1219–1227, May 2019.

[25] H. Huerta, R. Osorio, and N. Vázquez, "Nonlinear robust control of a machine to make thin films," *Rev. Iberoamer. Autom. Inform. Ind.*, vol. 14, no. 3, pp. 246–255, 2017.

[26] A. J. Van der Schaft, *L_2-Gain and Passivity Techniques in Nonlinear Control*. London, U.K.: Springer-Verlag, 1999.

[27] P. C. Krause, O. Wasynczuk, and S. D. Sudhoff, *Analysis of Electric Machinery and Drive Systems*, 2nd ed. New York, NY, USA: IEEE Press, 2002.

[28] S. Fiaz, D. Zonetti, R. Ortega, J. Scherpen, and A. Van der Schaft, "On port-Hamiltonian modeling of the synchronous generator and ultimate boundedness of its solutions," in *Proc. 4th IFAC Workshop Lagrangian Hamiltonian Methods Non Linear Control*, Bertinoro, Italy, 2012, pp. 30–35.

HÉCTOR HUERTA was born in Guadalajara, Jalisco, México, in 1980. He received the B.S. degree in communications and electronics engineering from the Universidad de Guadalajara, in 2003, and the M.Sc. and Dr.Sc. degrees in electric engineering from the Centro de Investigación y de Estudios Avanzados (CINVESTAV), Guadalajara, in 2005 and 2008, respectively.

Since 2012, he has been with the Department of Computational Sciences and Engineering, Centro Universitario de los Valles, Universidad de Guadalajara. His research interests include sliding modes control, power electric systems control, and electric machines control.

NIMROD VÁZQUEZ (Senior Member, IEEE) was born in México City, México, in 1973. He received the B.S. degree in electronics engineering from the Instituto Tecnológico de Celaya, Celaya, México, in 1994, and the M.Sc. degree in electronics engineering and the Dr.-Ing. degree from the Centro Nacional de Investigación y Desarrollo Tecnológico (CENIDET), Cuernavaca, México, in 1997 and 2003, respectively.

Since 1998, he has been with the Department of the Electronics Engineering, Instituto Tecnológico de Celaya. His research interests include dc/ac converters, power-factor correction, nonlinear control techniques, and renewable energy.